Journal of Solid State Chemistry **156,** 26–31 (2001)
doi:10.1006/jssc.2000.8953, available online at http://www.idealibrary.com on IDEAL®

# Synthesis and Single-Crystal Growth of $Ca_{2-x}Sr_xRuO_4$

Satoru Nakatsuji* and Yoshiteru Maeno*,†

*Department of Physics, Kyoto University, Kyoto 606-8502, Japan; and †CREST, Japan Science and Technology Corporation, Japan

Received May 23, 2000; in revised form August 8, 2000; accepted September 5, 2000; published online December 21, 2000

**For the study of the quasi-two-dimensional Mott transition system $Ca_{2-x}Sr_xRuO_4$, we have succeeded in synthesizing polycrystalline samples and also growing single crystals by a floating-zone method. Details of the preparations for the entire solution range are described. The structural, transport, and magnetic properties of both polycrystalline and single-crystal samples are fully in agreement.** © 2001 Academic Press

***Key Words:*** **$Ca_{2-x}Sr_xRuO_4$; Mott transition; $Sr_2RuO_4$; $Ca_2RuO_4$; spin-triplet superconductor; Mott insulator; *p*-wave superconductivity; ruthenate; floating zone method; quasi-two-dimensional system.**

## INTRODUCTION

First synthesized in 1959 (1), $Sr_2RuO_4$ was known simply as a paramagnetic conductor, until its superconductivity was revealed in 1994 (2). Quite interestingly, it shares the same $K_2NiF_4$-type structure with one of the best-studied high transition temperature ($T_c$) superconductors $La_{2-x}Sr_xCuO_4$. In contrast with the spin-singlet *d*-wave paring in high-$T_c$ cuprates, it has recently been demonstrated that $Sr_2RuO_4$ is a spin-triplet superconductor (3).

The discovery of the superconductivity in $Sr_2RuO_4$ has stimulated searches for superconductivity in related new ruthenates (4, 5). The Ca analogue, $Ca_2RuO_4$, has recently been synthesized (5, 6). In contrast with the superconductive $Sr_2RuO_4$, $Ca_2RuO_4$ is a Mott insulator (5, 7, 8). Naively, it is expected that 4*d* electrons in the highly extended orbitals should have only a weaker correlation in comparison with the 3*d* case. Yet, the existence of this Mott insulator confirms that strong correlation plays a significant role in this 4*d*-electron system, and probably in the mechanism of the superconductivity in $Sr_2RuO_4$. To explore the correlation effects in the ruthenates, $Ca_{2-x}Sr_xRuO_4$ is an ideal system that should bridge a new type of the Mott-transition route between the Mott insulator $Ca_2RuO_4$ and the spin-triplet superconductor $Sr_2RuO_4$ (9). We have succeeded in synthesizing polycrystalline samples and in growing single crystals of this solid solution system.

In this paper, we will present details of the synthesis of polycrystalline samples and also the single-crystal growth of $Ca_{2-x}Sr_xRuO_4$ in the entire range of $x$. Especially for the preparation of the polycrystalline samples, we discuss the systematic change of reaction conditions, which require careful attention to tune the heating temperature and atmosphere for each $x$. The results of structural analysis by X-ray diffraction for both polycrystalline and single-crystalline samples agree well with each other. In addition, the consistency between polycrystalline and single-crystalline samples in transport and magnetic properties demonstrates that the intrinsic properties of $Ca_{2-x}Sr_xRuO_4$ can be well studied using polycrystalline samples.

## PREPARATION OF POLYCRYSTALS AND SINGLE CRYSTALS

The conditions for the synthesis of polycrystalline $Ca_{2-x}Sr_xRuO_4$ allow only a narrow window for the appropriate heating temperature and atmosphere that is heavily dependent on $x$. We synthesized polycrystalline $Ca_{2-x}Sr_xRuO_4$ from $CaCO_3$(purity 4N), $SrCO_3$(4N), and $RuO_2$(3N) mixed in the stoichiometric proportion. The mixtures were pressed into 10-mm-diameter pellets under about 2000 kgf/cm$^2$. A tubular furnace, which allows controlled gas flow, was used for sintering. We explored heating temperatures between 1100 and 1570°C, and $O_2$ partial pressures between 0 and 0.01 bar in $Ar + O_2$ atmosphere with the total pressure of 1 bar. In order to minimize the evaporation of $RuO_2$ at high temperatures, we inserted pellets directly into a hot furnace, and after heating, pulled them out of the furnace hot and quenched them in air. Heating times of 12 and 16 h were employed, but they yielded no significant difference.

Figures 1a and 1b show the dependence of the major phase in a pellet on the reaction temperature after an initial heating in a 99% Ar + 1% $O_2$ atmosphere and a 99.9% Ar + 0.1% $O_2$ atmosphere, respectively. The stability range of $Ca_{2-x}Sr_xRuO_4$ (214 phase) changes remarkably with oxygen partial pressure. Furthermore, even in the same atmosphere, we see the significant and systematic variations of the stable temperature range with $x$ for the 214 phase.



0022-4596/01 $35.00

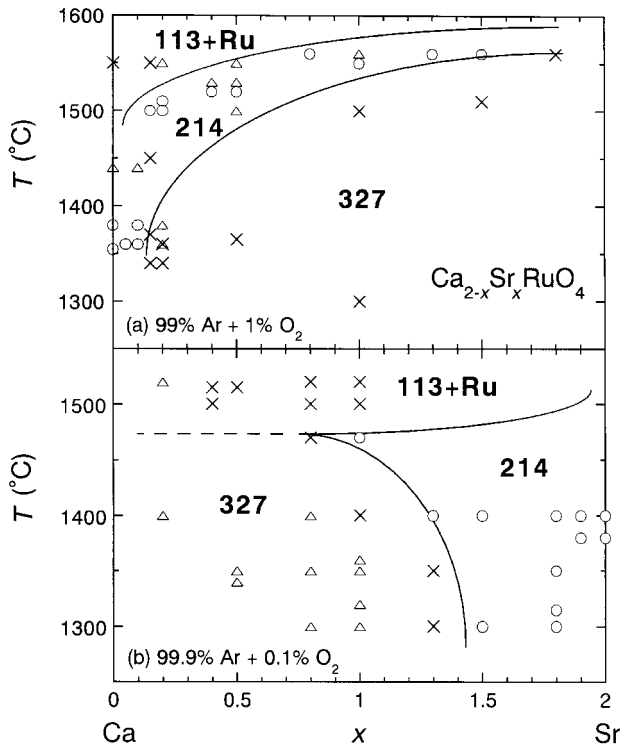


**FIG. 1.** Major phases in polycrystalline pellets as a function of the heating temperature and the Sr concentration $x$ under the atmosphere of (a) 99% Ar + 1% $O_2$ and (b) 99.9% Ar + 0.1% $O_2$. The circle, triangle, and cross indicate that the fraction of the 214 phase is approximately more than 80%, around 50%, and less than 30%, respectively. 327, 113, and Ru indicate that the dominant phase is $Ca_{3-x}Sr_xRu_2O_7$, $Ca_{1-x}Sr_xRuO_3$, and Ru metal, respectively. The solid and broken lines are guides to the eye.

Generally, the atmosphere becomes more reducing at higher temperatures as well as with decreasing oxygen partial pressure. Taking into account the physical phase diagram of magnetic and electrical properties described below, Figs. 1a and 1b suggest that the metallic 214 phase is more stable under relatively reducing conditions, reflecting the expected stronger covalency of the metallic Ru–O bond.

Although single-phase samples were obtained using both atmospheres, we sometimes had difficulty in obtaining well-sintered samples for the region $0.2 \leq x \leq 1.0$. This is most likely due to the heavy evaporation of $RuO_2$ under rather high heating temperatures as in Figs. 1a and 1b. In order to lower the temperature for the synthesis, we carefully investigated the atmosphere and temperature dependence of the major phase in pellets with $x = 0.2$, 0.4, 0.5, 0.8, and 1.0. Figure 2 presents the result for the case with $x = 1.0$.

The systematic change of the reaction temperature in Figs. 1a, 1b, and 2 indicates the following two competing aspects. First, while the metallic 214 phase may favor a rather reducing condition as noted above, too high a temperature and too strongly a reducing atmosphere prevents the formation of the 214 phase, but encourages the reduction of $RuO_2$ into Ru metal. Once Ru metal appears in a pellet, we have never succeeded in obtaining the 214 phase by repeating the same heating process. This condition determines the upper limit of the annealing temperature. Second, although the stoichiometric $Sr_2RuO_4$ and $Ca_2RuO_4$ can be obtained by annealing at relatively low temperature near 1300°C, the reaction temperature for the solution system $Ca_{2-x}Sr_xRuO_4$ increases as the Sr content $x$ approaches 1. Instead the $Ca_{3-x}Sr_xRu_2O_7$ (327) phase becomes stable up to a higher temperature, which may be correlated with the additional diffusion process to mix Ca and Sr in the solution system, in contrast with the endmembers ($x = 0$ and 2.0).

On the basis of a series of phase diagrams including Figs. 1 and 2, we have established the $x$ dependence of the optimized reaction temperature and atmosphere, as summarized in Table 1. Grinding and sintering were repeated several times to obtain more homogeneous samples with better crystallinity. As mentioned above, we introduced pellets into a hot furnace at an appropriate temperature, and after heating, quenched them to room temperature. This procedure also helps avoid the inclusion of $Ca_{1-x}Sr_xRuO_3$ (113) phase and/or 327 phase. However, to obtain well-sintered samples, we noticed that it is better to first synthesize a mixed phase of 214 with a little amount of 327 as a precursor, by reacting the raw material at a temperature slightly lower (by about 50°C) than the stable one for 214. This preceding treatment yielded better sintered samples.

Contamination of samples was minimized. In particular, Ca in a sample readily reacts with an $Al_2O_3$ crucible and

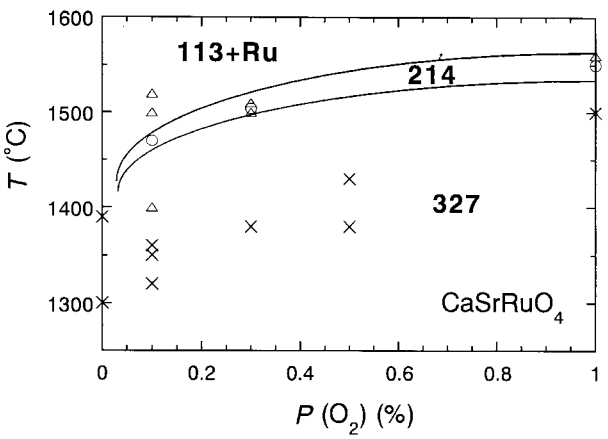


**FIG. 2.** Major phases in polycrystalline pellets as a function of the reaction temperature and the oxygen partial pressure $P(O_2)$ in the mixture of Ar and $O_2$ with the total pressure of 1bar. The nominal composition is $CaSrRuO_4$ ($x = 1.0$). The circle, triangle, and cross indicate that the fraction of the 214 phase is approximately more than 80%, around 50%, and less than 30%, respectively. The solid lines are guides to the eye.

**TABLE 1**
**Optimized Reaction Temperature and Atmosphere for Polycrystalline $Ca_{2-x}Sr_xRuO_4$, with Various Values of $x$**

| $x$ | Temperature(°C) | Atmosphere |
|---|---|---|
| 0.00[5] | 1360–1380 (1360) | $Ar + O_2$ 1.0% |
| 0.05 | 1320–1340 (1340) | $Ar + O_2$ 1.0% |
| 0.10 | 1360–1380 (1380) | $Ar + O_2$ 1.0% |
| 0.15 | 1360 (1360) | $Ar + O_2$ 0.3% |
| 0.20 | 1380–1395 (1380) | $Ar + O_2$ 0.3% |
| 0.25 | 1400–1410 (1410) | $Ar + O_2$ 0.3% |
| 0.40 | 1520 (1520) | $Ar + O_2$ 1.0% |
| 0.50 | 1520 (1520) | $Ar + O_2$ 1.0% |
| 0.80 | 1500–1505 (1505) | $Ar + O_2$ 0.3% |
| 1.00 | 1503 (1503) | $Ar + O_2$ 0.3% |
| 1.30 | 1380–1400 (1400) | $Ar + O_2$ 0.1% |
| 1.50 | 1300–1400 (1400) | $Ar + O_2$ 0.1% |
| 1.80 | 1300–1400 (1400) | $Ar + O_2$ 0.1% |
| 1.90 | 1300–1400 (1400) | $Ar + O_2$ 0.1% |
| 2.00 | 1100–1400 (1400) | $Ar + O_2$ 0.1% |

*Note.* For the final sintering, the samples were heated at the temperatures indicated in parentheses.

forms an eutectic Ca–Al–O compound with a melting point lower than 1300°C. In order to avoid this reaction as well as the contamination by diffusion of impurities, we placed two or three pellets of the same composition on top of a pellet of $Sr_2RuO_4$ in an $Al_2O_3$ crucible, and used only the top of the two or the middle of the three for measurements.

We have recently succeeded in growing single crystals of $Ca_{2-x}Sr_xRuO_4$ in the whole region of $x$ by a floating zone method with Ru self-flux. As in the polycrystalline sample preparation, we first made a pellet from a mixture of $CaCO_3$, $SrCO_3$, and $RuO_2$. Here, the volatility of $RuO_2$ is also a serious problem. To compensate for this loss, we prepared a Ru-rich starting material with a composition of $Ca_{2-x}Sr_xRu_{1.15}O_4$. After presynthesizing the pellet, we ground it again and pressed it under a pressure of 1500 kgf/cm$^2$ into a rod of 6–8 cm in length and about 5 mm in diameter. The rod was sintered at 1000°C for 12 h in air. Contamination was avoided, especially during the heating. We took the same precautions as for the polycrystalline samples described above.

In the floating zone method, the focused infrared radiation melts the rod without any physical contact with a crucible, so that no contamination is expected during the crystal growth. We used a commercial infrared image furnace (NEC Machinery, Model SC-K15HD) and performed the crystal growth typically under a 90% Ar + 10% $O_2$ gas mixture with a total pressure of 10 bar and a growth speed of 20 mm/h. The average size of single crystals obtained so far is about $5 \times 3 \times 3$ mm$^3$, still substantially smaller than those of $Sr_2RuO_4$. Details of the single-crystal growth of the superconductor $Sr_2RuO_4$ is presented elsewhere (10).

## STRUCTURAL ANALYSIS

The crystal structures at room temperature of both polycrystalline and single-crystalline samples were studied by powder X-ray (Cu$K\alpha$) diffraction measurements. In Fig. 3, we summarize the results of polycrystalline $Ca_{2-x}Sr_xRuO_4$ synthesized under the condition listed in Table 1. All of the X-ray spectra are basically consistent with $K_2NiF_4$-type structure and well indexed with tetragonal symmetry in the region $0.2 \leq x \leq 2$, and with orthorhombic symmetry in the region $0 \leq x < 0.2$. Each sample is revealed to be a single phase, except for a small inclusion of CaO probably due to the evaporation of $RuO_2$. The results for the single-crystalline samples show spectra essentially identical to those for the polycrystalline samples. Moreover, for the case of the single crystals, no impurity phase was detected for the entire range of Sr contents.

In order to clarify the systematic variation of the cell parameters, we considered here a unit cell with I4/*mmm* like that of $Sr_2RuO_4$ for the tetragonal lattice, while in the region $0 \leq x < 0.2$, we show $a = a_o/\sqrt{2}$ and $b = b_o/\sqrt{2}$, where $a_o$ and $b_o$ are the in-plane cell parameters for the orthorhombic unit cell as in Ref. (11). The cell parameters based on this assignment are plotted in Fig. 4. The solid and open squares correspond to the single-crystal and polycrystalline samples, respectively. Parameters of the single crystals were displayed using the Sr content of the starting materials. They agree well with those of the polycrystalline samples, which confirms the homogeneous mixing of Ca and Sr. The volume increases almost linearly with $x$ reflecting the larger size of $Sr^{2+}$ than of $Ca^{2+}$. In the region $0 \leq x \leq 0.2$, however, the cell parameters $a$ and $b$ split and decrease with $x$, while $c$ increases rapidly. These changes

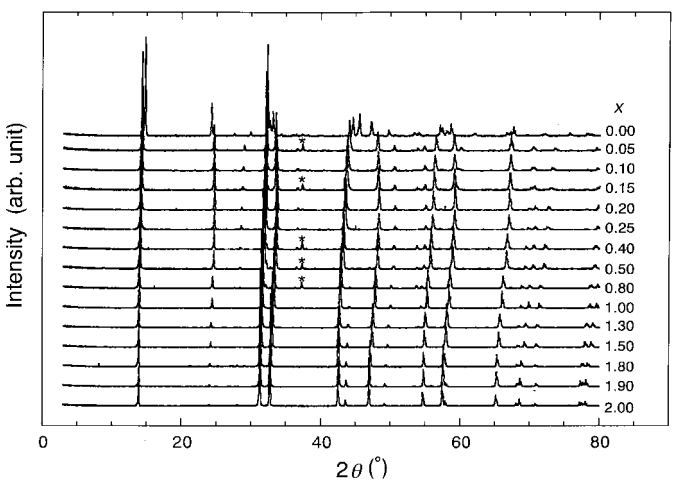


**FIG. 3.** X-ray diffraction spectra at room temperature of polycrystalline $Ca_{2-x}Sr_xRuO_4$ for various Sr concentrations $x$. The asterisk indicates a small inclusion of CaO.

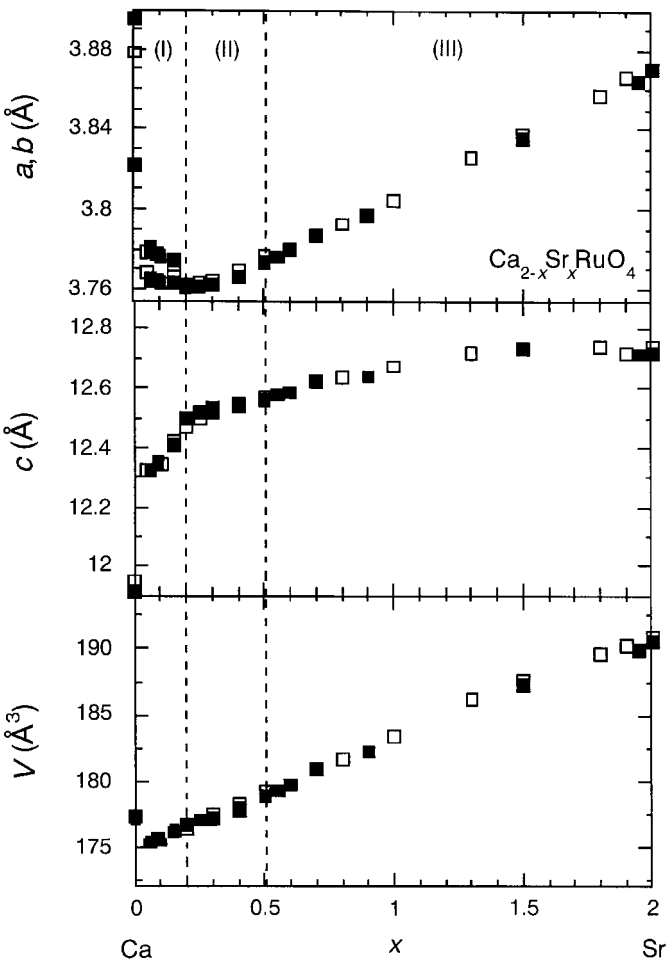


**FIG. 4.** Cell parameters $a$, $b$, $c$ and unit cell volume $V$ of $Ca_{2-x}Sr_xRuO_4$ against the Sr concentration $x$ of their starting materials. The open and solid squares respectively represent those of polycrystalline and single-crystalline samples.

indicate that a structural transition between an orthorhombic phase and a tetragonal phase occurs at around $x = 0.2$ and room temperature.

The structures of the endmembers have previously been determined by neutron diffraction measurements (11, 12). $Ca_2RuO_4$ has a highly distorted $K_2NiF_4$ structure with both rotation and tilt of the $RuO_6$ octahedra (11). On the other hand, $Sr_2RuO_4$ exhibits neither rotational nor tilt distortion (12), although phonon dispersion measurements have indicated that it is close to a rotational instability (13). Given these results, it is naturally expected that Ca substitution in $Sr_2RuO_4$ first stabilizes the rotation of $RuO_6$ octahedra in the region $2.0 > x \geq 0.2$. In fact, the occurrence of the maximum in the $c$-axis parameter at $x = 1.5$ is suggestive of the onset of the static rotational distortion. The large reduction in the $c$ parameter across the structural transition near $x = 0.2$ marks the onset of additional tilt. Recent neutron diffraction measurements at room temperature have indeed confirmed that these simple expectations are correct in this system (14).

## PHYSICAL PHASE DIAGRAM

Here, we briefly review the phase diagram of the physical properties of $Ca_{2-x}Sr_xRuO_4$ (9), which consists of the following three regions:

I. $0 \leq x < 0.2$. Insulating phase with canted antiferromagnetic ordering appears at low temperatures, in contrast with paramagnetic metal phase at high temperatures. Therefore, a metal/nonmetal transition occurs by varying temperature. $Ca_2RuO_4$ ($x = 0$) is the Mott insulator up to 350 K (8, 14).

II. $0.2 \leq x \leq 0.5$. Antiferromagnetically correlated metallic region (we call this "magnetic metallic region") appears at low temperatures.

III. $0.5 < x \leq 2.0$. Paramagnetic metallic phase spreads in this wide region. Itinerant magnetism changes continuously with $x$ from Curie–Weiss like paramagnetism to Pauli paramagnetism at $x = 2.0$. Superconductivity occurs at $x = 2.0$ below $T_c = 1.5$ K.

## ELECTRICAL PROPERTIES OF POLYCRYSTALLINE SAMPLES

We measured the resistivity of polycrystalline samples by a standard four-probe method. The resistivity curves $\rho(T)$ for the region I measured on cooling are shown in Fig. 5. For $x = 0$, $Ca_2RuO_4$ shows insulating behavior as a Mott insulator. However, a small Sr substitution for Ca dramatically changes the temperature dependence of the resistivity. For $x = 0.05$, 0.10 and 0.15, $\rho(T)$ is almost constant at high temperatures like the metallic $Sr_2RuO_4$. Below some characteristic temperature $T_{M/NM}$, however, the temperature dependence suddenly changes into an insulating one. This change indicates that a metal/nonmetal (M/NM) transition occurs on cooling at this point. The inset of Fig. 5 illustrates thermal hysteresis observed in $\rho(T)$ for $x = 0.15$, which confirms that the transition is of the first order. The transition temperature $T_{M/NM}$ was determined from the intersection of the extrapolations of low- and high-temperature $\log\rho$–$T$ curves measured on cooling. $T_{M/NM}$ decreases rapidly with $x$, and finally becomes zero at around $x = 0.2$. All of the observations here are consistent with those for the single-crystalline samples (9).

Figure 6 shows the resistivity data for polycrystalline samples in regions II and III. For comparison, we also show the data for $x = 0.15$. In contrast with the insulating $Ca_2RuO_4$, the $\rho(T)$ curves in regions II and III have small absolute values and little temperature dependence. Even for a good metal such as $Sr_2RuO_4$ (the in-plane resistivity $\rho_{ab} \approx 120\ \mu\Omega$cm and the out-of-plane resistivity $\rho_c \approx$

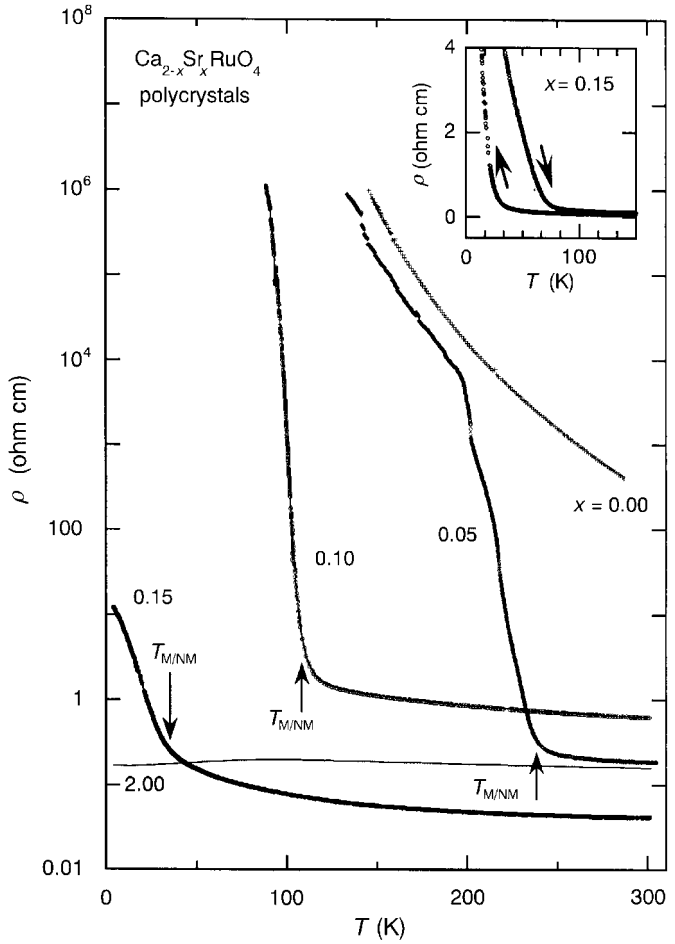


**FIG. 5.** Temperature dependence of the resistivity $\rho(T)$ on cooling for the region I ($0 \leq x \leq 0.2$) of polycrystalline $Ca_{2-x}Sr_xRuO_4$. $T_{M/NM}$ is the metal/nonmetal transition temperature. The inset shows the hysteresis in $\rho(T)$ for $x = 0.15$.

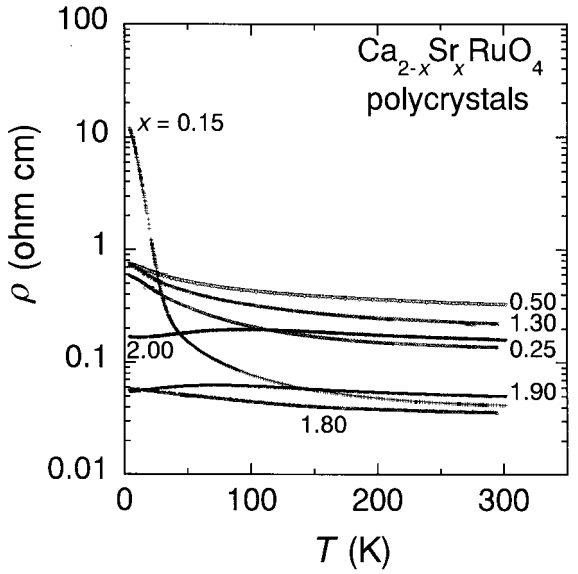


**FIG. 6.** Temperature dependence of the resistivity $\rho(T)$ on cooling for $0.15 \leq x \leq 2.0$ of polycrystalline $Ca_{2-x}Sr_xRuO_4$.

30 mΩcm at 300 K), the polycrystalline sample shows almost temperature independence and at high temperatures weakly semiconducting resistivity. This difference between the data for single-crystal and polycrystalline samples is attributable to poor conduction of the grain boundaries (2). Taking this into account, the intrinsic behavior of the region $0.2 \leq x \leq 2.0$ may well be metallic at all the temperatures. To confirm this, we measured $\rho_{ab}$ of single-crystal samples with $x = 0.2$, 0.5, 0.9, 1.5, and 2.0. Indeed, all of them show metallic temperature dependence with positive $d\rho/dT$ at all the temperatures (15). On the other hand, $\rho_c$ in this system is almost temperature independent and sometimes shows nonmetallic behavior, reflecting the quasi-two-dimensional structure (15). Therefore, in addition to the resistance of its grain boundary material such as CaO or SrO, as discussed in Ref. (16), this highly anisotropic transport property should also be responsible for the weakly semiconductive behavior of polycrystalline samples. In fact, a broad peak at around 100 K for $x = 2.00$ in Fig. 6 is most probably reflecting the maximum in $\rho_c$ (2). Given these effects, the observed temperature independence or weekly semiconducting behavior in polycrystalline samples is considered consistent with the transport properties observed in the single crystals.

Finally, we note the fact that the magnetic properties of both the polycrystalline and single-crystalline samples also agree qualitatively and even quantitatively well with each other. The absolute values of the susceptibility and its temperature dependence show identical behavior to each other in all the regions, as shown in Fig. 4 of Ref. (9) and Fig. 7 of Ref. (15). This consistency in the measured physical properties between polycrystalline and single-crystalline samples demonstrates that we are able to deduce the intrinsic properties of this system by investigating the polycrystalline samples.

## CONCLUSION

We describe the syntheses of polycrystalline samples and also of single crystals of the quasi-two-dimensional Mott transition system $Ca_{2-x}Sr_xRuO_4$ for the entire region of $x$. We report the details of their preparations. Especially for the polycrystalline samples, we discuss the systematic change of the reaction conditions, which requires careful tuning of the heating temperature and atmosphere for each concentration, $x$. The results of a structural analysis on both polycrystalline and single-crystalline samples show excellent agreement. Moreover, measurements of transport and magnetic properties of polycrystals and single crystals demonstrate that polycrystalline samples are suitable for investigations of the intrinsic properties of this system.

## ACKNOWLEDGMENTS

The authors acknowledge T. Ishiguro for his support. They thank T. Ando, H. Fukazawa, and M. Minakata for their technical support and valuable discussions. This work has been supported in part by a Grant-in-Aid for Scientific Research on Priority Areas from the Ministry of Education, Science, Sports and Culture of Japan. One of the authors (S.N.) has been supported by JSPS Research Fellowships for Young Scientists.

## REFERENCES

1. J. J. Randall and R. Ward, *J. Am. Ceram. Soc.* **81,** 2629 (1959).
2. Y. Maeno, H. Hashimoto, K. Yoshida, S. Nishizaki, T. Fujita, J. G. Bednorz, and F. Lichtenberg, *Nature* **372,** 532 (1994).
3. K. Ishida, H. Mukuda, Y. Kitaoka, K. Asayama, Z. Q. Mao, Y. Mori, and Y. Maeno, *Nature* **396,** 658 (1998).
4. S. Ikeda, Y. Maeno, and T. Fujita, *Phys. Rev. B* **57,** 978 (1998).
5. S. Nakatsuji, S. Ikeda, and Y. Maeno, *J. Phys. Soc. Jpn.* **66,** 1868 (1997).
6. G. Cao, S. McCall, M. Shepard, J. E. Crow, and R. P. Guertin, *Phys. Rev. B* **56,** R2916 (1997).
7. H. Fukazawa, S. Nakatsuji, and Y. Maeno, *Physica B* **281/282,** 613 (2000).
8. C. S. Alexander, G. Cao, V. Dobrosavljevic, S. McCall, J. E. Crow, E. Lochner, and R. P. Guertin, *Phys. Rev. B* **60,** R8422 (1999).
9. S. Nakatsuji and Y. Maeno, *Phys. Rev. Lett.* **84,** 2666 (2000).
10. Z. Q. Mao, Y. Maeno, and H. Fukazawa, *Matt. Res. Bull.* **35** (2000), in press.
11. M. Braden, G. André, S. Nakatsuji, and Y. Maeno, *Phys. Rev. B* **58,** 847 (1998).
12. M. Braden, A. H. Moudden, S. Nishizaki, Y. Maeno, and T. Fujita, *Physica C* **273,** 248 (1997).
13. M. Braden, W. Reichardt, S. Nishizaki, Y. Mori, and Y. Maeno, *Phys. Rev. B* **57,** 1236 (1998).
14. O. Friedt, M. Braden, S. Nakatsuji, and Y. Maeno, submitted for publication.
15. S. Nakatsuji and Y. Maeno, *Phys. Rev. B* **62,** 6458 (2000).
16. R. J. Cava, H. W. Zandbergen, J. J. Krajewski, W. F. Peck, Jr., B. Batlogg, S. Carter, R. M. Fleming, O. Zhou, and L. W. Rupp, Jr., *J. Solid State Chem.* **116,** 141 (1995).